Magnetohydrodynamic equilibrium and stability of fieldreversed configurations

J. L. Schwarzmeier, D. C. Barnes, D. W. Hewett, C. E. Seyler, A. I. Shestakov, and R. L. Spencer

Citation: Physics of Fluids (1958-1988) **26**, 1295 (1983); doi: 10.1063/1.864290
View online: http://dx.doi.org/10.1063/1.864290
View Table of Contents: http://scitation.aip.org/content/aip/journal/pof1/26/5?ver=pdfcov
Published by the AIP Publishing

Magnetohydrodynamic equilibrium and stability of field-reversed configurations

J. L. Schwarzmeier, D. C. Barnes,[a] D. W. Hewett,[b] C. E. Seyler,[c] A. I. Shestakov,[d] and R. L. Spencer
Los Alamos National Laboratory, University of California, Los Alamos, New Mexico 87545

(Received 10 September 1982; accepted 13 January 1983)

Magnetohydrodynamic equilibrium and stability studies of field-reversed configurations are presented. Experimentally realistic equilibria are calculated numerically for a plasma inside a conducting cylinder. Stability studies indicate that equilibria ranging from elliptical to highly racetrack-shaped are all unstable to the internal tilting mode.

I. INTRODUCTION

Field-reversed configurations (FRC's) experimentally have exhibited remarkable stability on the magnetohydrodynamic (MHD) timescale,[1–3] despite numerous MHD calculations showing FRC's to be unstable.[4–11] Analytical calculations using linearized MHD theory show that the equilibria should be very unstable to perturbations of the localized co-interchange type (also called ballooning modes) in which the toroidal mode number n approaches infinity.[4,5] However, a quantitatively accurate description of local modes should involve an ion kinetic description of the plasma dynamics and would almost certainly show that finite-Larmor-radius effects greatly suppress the growth rates.[12] More puzzling are linear calculations using equilibria with elliptical flux surfaces showing that such equilibria also are quite unstable to the global $n = 1$ tilting mode,[6–11] where ion kinetic effects should be much less stabilizing. The possibility that the unstable tilting mode might saturate at a low level due to nonlinear effects was investigated in an ideal nonlinear MHD simulation.[9] The simulation code was initialized with an elliptical equilibrium and showed that the tilting mode did not saturate at low amplitude.

Three remaining possibilities for explaining the observed stability of the tilting mode are: (1) ion kinetic effects *are* important even though it is a global mode; (2) there are nonelliptical equilibria that are stable to the tilting mode within MHD; and (3) nonelliptical equilibria, though unstable, saturate at low amplitude. In this paper we discuss the second of these possibilities. In previous calculations of the tilting instability, elliptical flux surfaces were used although analytical work on FRC stability has indicated that equilibrium profile effects could be a strong factor in determining tilt stability. Furthermore, the experiments strongly suggest that the flux surfaces are not elliptical but are rather more racetrack-like in shape.[1] This suggests that we simply need to generate experimentally realistic (i.e., racetrack flux surfaces inside a conducting cylinder) equilibria and analyze them for tilt stability. The equilibrium portion of this program has turned out to be very troublesome, but recently the difficulty was understood and overcome in a special case.[13] That work has now been generalized to allow the computation of elongated racetrack-like equilibria with arbitrary pressure profiles.[14] The purpose of the present work is to determine whether or not there exist experimentally realistic FRC equilibria that are stable to the global MHD tilting mode.

II. EQUILIBRIUM

Recently it became possible to solve for FRC equilibria with a wide variety of flux surface shapes and with flux surfaces outside the separatrix that satisfy experimental conditions.[13,14] In these calculations the Grad–Shafranov equation for the case of no toroidal field,

$$\Delta^* \psi = -r^2 \frac{dP}{d\psi}, \qquad (1)$$

is solved with the boundary conditions that ψ is a constant on a cylindrical conducting wall of radius r_{wall} and that $\partial\psi/\partial z = 0$ at the ends of the cylindrical conducting region. It is convenient to represent the pressure profile in the form $P(\psi) = cf(\psi)$, where f is a bounded shape function; c thus determines the magnitude of the right-hand side of Eq. (1). The equilibrium is specified by choosing the total current in the computational region; c is determined as part of the solu-

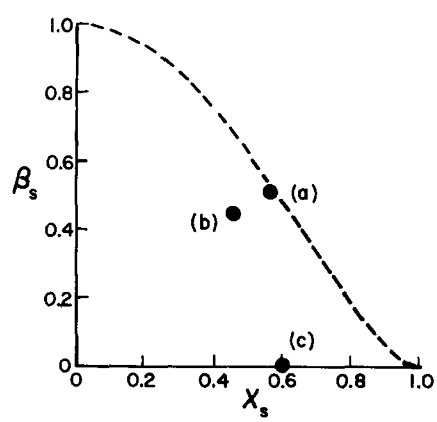

FIG. 1. β_s vs x_s, showing the equilibrium boundary for the numerical equilibria with realistic cylindrical boundary conditions. The three equilibria (a), (b), and (c) are shown in Fig. 2.

[a] Current address: Institute for Fusion Studies, University of Texas, Austin, Texas 78712.
[b] Current address: Plasma and Fusion Center, MIT, 167 Albany St., Cambridge, Massachusetts 02139.
[c] Current address: Laboratory of Plasma Studies and School of Electrical Engineering, Cornell University, Ithaca, New York 14853.
[d] Current address: Lawrence Livermore National Laboratory, University of California, Livermore, California 94550.

tion. Solutions are ultimately obtained by combining the toroidal current constraint with an adaptive iteration procedure.[14]

Guided by the results of experiments, we specialize to shape functions, $f(\psi)$, that are monotonic in ψ between the separatrix and the vortex point and that rapidly fall to zero outside the separatrix, representing loss of plasma along open field lines. The effect of different choices for the pressure profile is studied with a one-dimensional radial equilibrium code that takes a shape function f with two free parameters in it and varies them, together with c, until it produces a one-dimensional equilibrium satisfying the average-beta condition[1,6] and having specified values of $x_s = r_{sep}/r_{wall}$ and $\beta_s = P_{sep}/P_{max}$.[14] This facilitates comparison with the experiment since these are inferred quantities. This profile, with the value of c as an initial guess, is then used in the two-dimensional equilibrium code. A shape function which successfully produces a wide variety of combinations of x_s and β_s is the function $f(\psi) = \tanh(a\psi + b)$. Figure 1 shows the region of the x_s-β_s space containing equilibria with this $f(\psi)$. Beyond the boundary in this figure the average-beta condition can no longer be satisfied and no elongated equilibria exist. We have tried other shape functions that are consistent with the experimental constraints and the position of the equilibrium boundary is hardly changed; the boundary in Fig. 1 thus seems to be generic to FRC's. Point (b) in Fig. 1 corresponds to typical shots from the Los Alamos experiments FRX-B and FRX-C. Figure 2 shows three flux plots from the two-dimensional equilibrium code. All three have an elongation of about five. Note that the equilibrium near the equilibrium boundary has rather elliptical flux surfaces while the one with a small value of β_s has quite racetrack-shaped flux surfaces.

III. STABILITY CODES

To address the question of stability we use two different methods: a trial function approach[12] for the magnetohydrodynamic potential energy δW, and a time-dependent, linearized MHD code.[7,15] In the first method the form of the trial function is of course a crucial aspect of the problem, since in general this approach gives only a necessary condition for stability. Let $\xi = (\xi_n, \xi_\theta, \xi_\parallel)$ denote the normal, azimuthal, and parallel displacements of the fluid with respect to the equilibrium magnetic field. The form of the perturbation we choose is that of a rigid incompressible axial displacement of the magnetic field lines in the (r,z) plane; the θ displacement is determined from incompressibility. We assume the azimuthal variation is $\exp(in\theta)$. In the (r,z) plane we take

$$\xi_n(\psi,\chi) = -\hat{B}_r(\psi,\chi)\xi_z(\psi), \qquad (2)$$

$$\xi_\parallel(\psi,\chi) = \hat{B}_z(\psi,\chi)\xi_z(\psi), \qquad (3)$$

where $\hat{B}_r = B_r/B$ and $\hat{B}_z = B_z/B$. Flux surfaces are denoted by ψ, and χ is the coordinate along $\mathbf{B}$. This form of the perturbation has been shown to lead to the tilting instability for highly elongated equilibria in which the flux surfaces, $\psi(r,z) =$ constant, are primarily elliptical in shape.[6,8] In addition, this form for ξ was shown to be the minimizing MHD displacement for localized co-interchange modes near the vortex point (magnetic axis).[4] Consequently we believe that this form of the perturbation is close to the general minimizing ξ for highly elongated elliptical equilibria.

The fact that the axial shift is rigid means that $\xi_z(\psi,\chi)$ is replaced by $\xi_z(\psi)$. Thus we are using a trial function approach only in the variable χ; the ψ dependence of ξ_z is determined by solving the normal mode equation. When we substitute the trial function form into the usual MHD δW we are

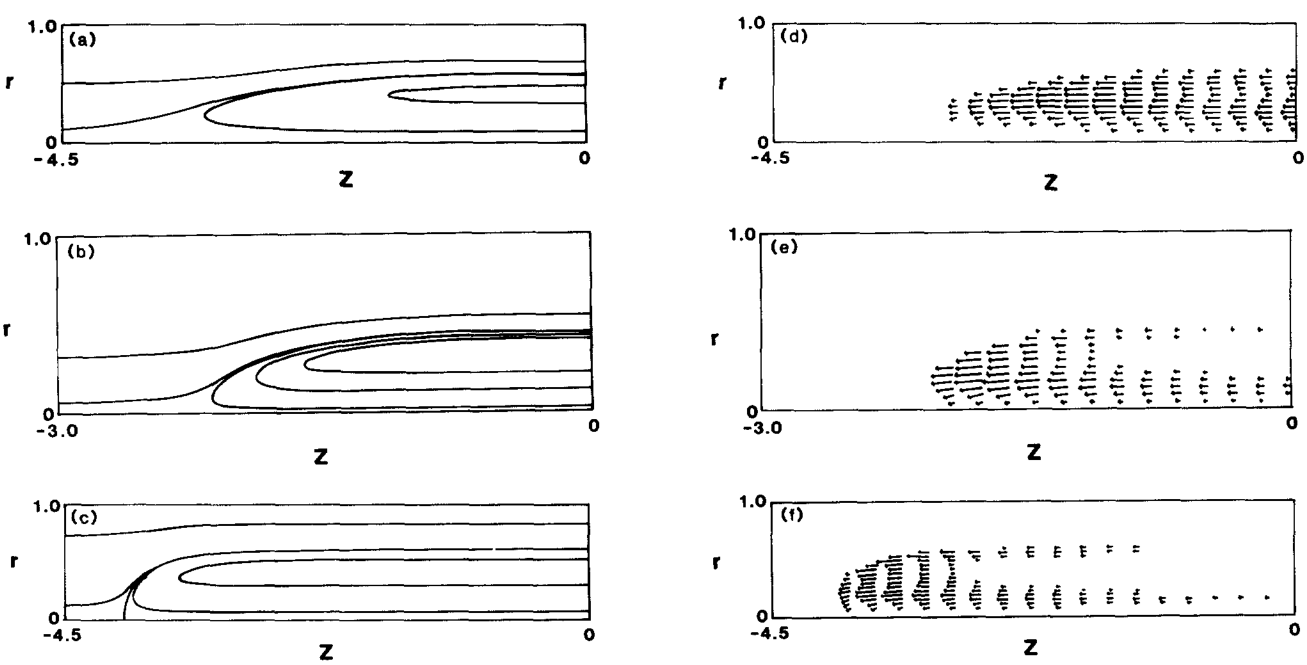

FIG. 2. Realistic numerical equilibria: (a) $\beta_s = 0.5$ and $x_s = 0.59$, (b) $\beta_s = 0.44$ and $x_s = 0.47$ (this corresponds to FRX-B parameters), and (c) $\beta_s = 0.01$ and $x_s = 0.6$. For each equilibrium (a)–(c), in (d)–(f) are shown the corresponding projections of the displacement vector ξ in the (r,z) plane from the initial value code.

led to a second-order ordinary differential equation to solve for $\xi_z(\psi;\omega)$ where ψ is the independent variable and ω is the unknown eigenfrequency. The domain in ψ is $[\psi_{\rm vor},0]$, where $\psi_{\rm vor}$ is the value of ψ at the vortex point and $\psi = 0$ at the separatrix. We choose as one boundary condition that $\xi_z(\psi = 0) = 0$. This states that the tilting instability is an internal mode, since the mode is confined to the closed field line region. One justification for this boundary condition comes from the MHD initial value code, where it is observed that the amplitude of the tilting mode always becomes very small at the separatrix [see Figs. 2(d)–2(f)]. The second boundary condition on $\xi_z(\psi)$ is a regularity condition that excludes the solution ξ_z that becomes singular at $\psi_{\rm vor}$. In the numerical implementation, $\xi_z(\psi;\omega)$ is expanded as

$$\xi_z(\psi;\omega) = \sum_{n=1}^{N} a_n(\omega)\eta_n(\psi) . \quad (4)$$

The basis functions $\{\eta_n\}$ are chosen to be cubic b splines, and the coefficients $a_n(\omega)$ are found by solving the homogeneous dispersion matrix problem that results. The eignfrequency ω is determined by requiring that the determinant of the dispersion matrix vanish as a function of ω.

In the second stability approach, the time-dependent resistive MHD equations are linearized about an equilibrium. The numerical methods used are very similar to those discussed in Ref. 15 (see especially Sec. 6.2). Equilibria symmetric about $z = 0$ give symmetric systems of equations, hence symmetric perturbations. Consequently, the domain of computation is: $0 \leqslant r \leqslant r_{\rm wall}$ and $0 \leqslant z \leqslant z_{\rm max}$. The only boundary conditions on the modes are set at the radial walls; symmetry conditions are imposed on the other three sides. The fastest growing mode is one in which the axial displacement is even about $z = 0$, while the radial one is odd, i.e., the tilting mode.

IV. RESULTS

We examine four equilibria: E1, a Hill's vortex solution that does not satisfy conducting-wall boundary conditions, and E2–E4, which do satisfy conducting-wall boundary conditions. The equilibria E2, E3, and E4 are those labeled as (a), (b), and (c), respectively, in Fig. 2. For E1 the pressure profile is $p(\psi) = cH(\psi)$, where H is the Heaviside function, and for E2–E4 $p(\psi) = (cd/a)[\tanh(a+b+e) - \tanh(a\psi + e\psi^3 + b)]$ (note that $\psi = 1$ at the conducting wall). The equilibrium parameters are summarized in Table I.

TABLE I. Parameters of the equilibria E1–E4. The pressure profile is given by $p(\psi) = (cd/a)[\tanh(a+b+e) - \tanh(a\psi + e\psi^3 + b)]$. $B_{z,\rm wall}$ is the field strength at $r = r_{\rm wall}$ and $z = 0$ used to calculate the normalizing field $\langle B \rangle$. $\langle n \rangle$ is the peak number density used to calculate the characteristic $\langle \rho \rangle$ of the deuterium plasma. τ_H is the Alfven time $[= a(4\pi\langle\rho\rangle)^{1/2}/\langle B\rangle$, where a is the necessary characteristic distance in order that $r_{\rm wall} = 12.5$ cm].

	E1	E2	E3	E4
a	···	7.976 4	36.563	30.546
b	···	0.299 97	0.135 6	1.120 5
c	···	37.368	47.37	28.45
d	···	0.744 55	1.302 4	2.725 5
e	···	0.0	19 211.0	0.0
$r_{\rm sep}/z_{\rm sep}$	0.227	0.133	0.214	0.148
x_s	0.47	0.59	0.47	0.6
β_s	0.0	0.5	0.44	0.01
$B_{z,\rm wall}$(kG)	5.0[a]	6.5	5.0	6.5
$\langle n\rangle 10^{15}$(cm^{-3})	1.16	3.36	1.14	3.36
τ_H(μsec)	0.064 8	2.27	1.4	2.26

[a] For E1, 5 kG is the field B_z at $z = 0$ and $r = r_{\rm sep}$.

TABLE II. Stability results from the initial value code for equilibria E1–E4. Mesh size gives the number of points ($N_r x N_z$) used to generate the equilibrium. S is the magnetic Reynolds number, $\tilde\gamma$ is the dimensionless growth rate, and $\tau_g = \tau_H/\tilde\gamma$ is the growth time.

Equilibrium	Mesh	S	$\tilde\gamma$	τ_g
E1	61× 81	10^4	0.060	1.08
E1	61× 81	10^5	0.06	1.1
E2	41× 81	10^2	0.7	3.0
E2	41× 81	10^3	0.7	3.0
E2	41× 81	10^4	0.75	3.0
E3	61× 81	10^3	1.63	0.86
E3	61× 81	10^4	1.63	0.86
E3	101×101	10^3	1.69	0.82
E4	81× 81	10^2	2.7	0.84
E4	81× 81	10^3	2.0	1.1
E4	101×101	10^3	1.8	1.3

In Table II we present stability results of the initial value code for the equilibria E1–E4. Dimensionless growth rates $\tilde\gamma$ (in terms of inverse Alfvén times) and growth times in microseconds τ_g (for typical FRX-B parameters) are presented for each equilibrium E1–E4 for various magnetic Reynolds numbers S and equilibrium mesh sizes $N_r x N_z$. The stability results are independent of S for large S, indicating that the tilting instability is an ideal mode. The table also shows that growth times independent of mesh size are obtained for sufficiently fine meshes. Not included in the table are runs showing that the shape of the resistivity profile also does not affect the growth rate.

The growth times from the trial function code for the equilibria E1–E4 are 1.1, 3.6, 4.2, and 22 μsec, respectively, to be compared to 1.1, 3, 0.86, and 1.3 μsec, respectively, from the initial value code. For elliptical equilibria (E1 and E2) the trial function code and the initial value code have growth rates that differ by about 10%, thus confirming the rigid axial shift assumption for the displacement. However, as the equilibria become more racetrack-like (E3 and E4) the initial-value code shows that the displacement is no longer rigid along a flux surface but becomes localized to the tip of the flux surface [see Figs. 2(d)–2(f)]. This is the same conclusion reached by Grossmann *et al.*[11] in the limit $n \to \infty$. Continuing to use the rigid axial displacement trial function for racetrack equilibria yields optimistic stability predictions with respect to growth rates, and can lead erroneously to regions of MHD stable equilibria. Depending on the shape of the eigenfunction $\xi_z(\psi;\omega)$, anywhere from $N = 10$ to $N = 100$ basis functions are required for convergence in Eq. (4).

V. DISCUSSION

The stability analyses show that all equilibria investigated are very unstable to tilting. For typical FRX-B operation using a deuterium plasma with $B_{\rm wall} = 5$ kG, $T = 540$

eV, $n_{max} = 1.14 \times 10^{15}$ cm^{-3}, $r_{wall} = 12.5$ cm, $x_s = 0.47$, and $r_{sep}/z_{sep} = 0.21$, we calculate the $n = 1$ mode growth time to be about $\gamma^{-1} \sim 0.9$ μsec. Such a rapidly growing global mode certainly should be observed in the experiments[1] where the lifetime is in the range 20 $\mu\text{sec} \leqslant \tau_{life} \leqslant 50$ μsec. In addition we find that the modes $n \geqslant 2$ always are significantly more unstable than the $n = 1$ mode.

For elliptical equilibria the axial shift of each flux surface is rigid to minimize field-line bending. In addition, an axial displacement has a nonzero component normal to the flux surface (i.e., down the pressure gradient) everywhere along its length (except at the midplane). However, for racetrack equilibria it is energetically more favorable to stretch the field lines by concentrating the displacement at the tips of the flux surfaces, since rigid axial displacements contribute nothing to δW along the long, straight sections of the flux surfaces. Since the displacements for racetrack equilibria are becoming localized (poloidally), the nonlinear behavior of these modes is an open question that needs to be resolved.

We have provided strong evidence that the stability of existing FRC's cannot be explained by the ideal MHD model. While we have not excluded the possibility that there exist realistic, stable MHD equilibria, we are reasonably confident that they do not exist. We currently are investigating the stability of FRC's to the tilting mode with a kinetic model[12] and will report on these results in a future publication.

ACKNOWLEDGMENT

This work was performed under the auspices of the U. S. Department of Energy.

[1] W. T. Armstrong, R. K. Linford, J. Lipson, D. A. Platts, and E. G. Sherwood, Phys. Fluids **24**, 2068 (1981).

[2] W. T. Armstrong, D. G. Harding, E. A. Crawford, and A. L. Hoffman (submitted to Phys. Fluids).

[3] A. G. Es'kov, R. Kh. Kurtmullaev, A. P. Kreshchuk, Ya. N. Laukhin, A. I. Malyutin, A. I. Markin, Yu. S. Martyushov, B. N. Mironov, M. M. Orlov, A. P. Proshletsov, V. M. Semenov, and Ya. B. Sosunov, in *Plasma Physics and Controlled Nuclear Fusion Research* (IAEA, Vienna, 1978), Vol. II, p. 187.

[4] W. A. Newcomb, Phys. Fluids **23**, 2296 (1980).

[5] J. R. Cary, Phys. Fluids **24**, 1818 (1981).

[6] D. C. Barnes, C. E. Seyler, and D. V. Anderson, in *Proceedings of the Symposium on Compact Toruses and Energetic Particle Injection* (Princeton U.P., Princeton, NJ, 1979), p. 110.

[7] A. I. Shestakov, D. D. Schnack, and J. Killeen, in *Proceedings of the Symposium on Compact Toruses and Energetic Particle Injection* (Princeton U. P., Princeton, NJ, 1979), p. 126.

[8] H. Weitzner (personal communication).

[9] D. C. Barnes, A. Y. Aydemir, D. V. Anderson, A. I. Shestakov, and D. D. Schnack, "Proceedings of the 3rd Symposium on the Physics and Technology of Compact Toroids in the Magnetic Fusion Energy Program," Los Alamos Report No. LA8700-C, Los Alamos, NM, 2–4 December, 1980.

[10] Yu A. Dreizin and E. P. Sokolov, Sov. J. Plasma Phys. **7**, 516 (1981).

[11] W. Grossmann, E. Hameiri, and H. Weitzner, Phys. Fluids **26**, 508 (1983).

[12] C. E. Seyler and D. C. Barnes, Phys. Fluids **24**, 1686 (1981).

[13] R. L. Spencer and D. W. Hewett, Phys. Fluids **25**, 1365 (1982).

[14] D. W. Hewett and R. L. Spencer, Phys. Fluids **26**, 1299 (1983).

[15] A. I. Shestakov, J. Killeen, and D. D. Schnack, J. Comp. Phys. **46**, 69 (1982).